RESEARCH ARTICLE
ATMOSPHERIC PHYSICS

Earth and Planetary Physics
9: 904–914, 2025
doi: 10.26464/epp2025022

Assessing historical snowfall patterns in Seoul from 1625 to 1907 CE in relation to the Grand Solar Minima

YuQi Wang[1], Yong Wei[1,2*], Feng Shi[3,4], ZhongHua Yao[5], ShiLing Yang[2,3], Wei Lin[1,2], LiMei Yan[1,2], Fei He[1,2], DaBang Jiang[6], XinAn Yue[1,2], Kai Fan[1,2], Si Chen[7], and YaoChen Yue[1,2]

[1]Center for Earth and Planetary Physics, Institute of Geology and Geophysics, Chinese Academy of Sciences, Beijing 100029, China;

[2]College of Earth and Planetary Sciences, University of Chinese Academy of Sciences, Beijing 100049, China;

[3]State Key Laboratory of Lithospheric and Environmental Coevolution, Institute of Geology and Geophysics, Chinese Academy of Sciences, Beijing 100029, China;

[4]CAS Center for Excellence in Life and Paleoenvironment, Beijing 100044, China;

[5]Department of Earth Sciences, The University of Hong Kong, Hong Kong 999077, China;

[6]Institute of Atmospheric Physics, Chinese Academy of Sciences, Beijing 100029, China;

[7]Aerospace Information Research Institute, Chinese Academy of Sciences, Beijing 100094, China

Key Points:
- The snowfall database in Seoul from 1625 to 1907 CE was compiled.
- The ASF (the annual snowfall frequency) decreased significantly and the FDS (the first date of annual snowfall) was notably postponed during the Maunder and Dalton minima.
- An 8- to 9-year cycle replaced the 11-year cycle in snowfall around both the Maunder and Dalton Minima.

Citation: Wang, Y. Q., Wei, Y., Shi, F., Yao, Z. H., Yang, S. L., Lin, W., Yan, L. M., He, F., Jiang, D. B., … Yue, Y. C. (2025). Assessing historical snowfall patterns in Seoul from 1625 to 1907 CE in relation to the Grand Solar Minima. *Earth Planet. Phys.*, *9*(4), 904–914. http://doi.org/10.26464/epp2025022

Abstract: The Sun is the primary energy source driving the Earth's climate system. A prevailing hypothesis suggests that even minor variations in solar activity, when amplified by climate system feedback mechanisms, can induce significant climatic changes on decadal to centennial timescales. However, the limited availability of historical winter climate proxies has impeded consensus on how solar variability influences the long-term winter climate in Northeast Asia, particularly during Grand Solar Minima (GMs). In this study, we analyzed daily-resolution snowfall records in Seoul from 1625 to 1907 CE, derived from the Korean official historical chronicle Seungjeongweon Ilgi. This period encompasses both the Maunder Minimum (1645–1715 CE) and the Dalton Minimum (1790–1830 CE) of solar activity. Our findings indicate that during the GMs, the first date of annual snowfall (FDS) was delayed by approximately 10 days, and the average annual snowfall frequency (ASF) was reduced by half compared to non-GM periods. Additionally, while an 11-year solar cycle was evident in the ASF during non-GM periods, this cycle was replaced by a shortened 8- to 9-year cycle during the GMs. These variations suggest a differential regional climatic response to prolonged changes in solar activity, and provide historical insights that enhance our understanding of the potential impact of low solar activity on the winter climate in Northeast Asia.

Keywords: historical records; Grand Solar Minima; solar activity; regional snowfall

1. Introduction

Interpreting climate changes prior to the industrial age and projecting climate changes in the coming decades both require a comprehensive understanding of the climate's response to natural forcings (Lean, 2010). The Sun, serving as the principal energy source for the Earth system, represents a significant external climate forcing (Siscoe, 1978; Braun et al., 2005; Gray et al., 2010; Solanki et al., 2013). Solar radiation variability is one of the primary drivers of climate change on centennial to millennial timescales (Zhao XH et al., 2020, 2021). Numerous proxy records support the critical role of solar variability in influencing the regional climate in Asia, particularly by way of the hydrological cycle (Neff et al., 2001; Feng SN et al., 2023; Zhang YC et al., 2024). Recent studies have shown that a strong 11-year solar cycle can trigger resonant responses of the intrinsic dominant modes of East Asian winter monsoon (EAWM) variations, thereby generating significant decadal change signals (Jin C et al., 2019). In years with strong (weak) solar activity, precipitation in southern China during late winter (January–March) tends to increase (decrease) significantly, especially in the middle reaches of the Yangtze River. (Ma HD et

First author: Y. Q. Wang, Wangyq@mail.iggcas.ac.cn
Correspondence to: Y. Wei, weiy@mail.iggcas.ac.cn
Received 03 DEC 2024; Accepted 06 FEB 2025.
First Published online 12 MAR 2025.

al., 2019).

Records of direct solar observations date back nearly 400 years (Muñoz-Jaramillo and Vaquero, 2019), a timespan encompassing at least two famous Grand Minima (GMs): the Maunder Minimum from 1645 to 1715 CE, and the Dalton Minimum from 1790 to 1830 CE (Eddy, 1976; Wagner and Zorita, 2005). Despite a significant reduction in overall solar activity and a virtual disappearance of sunspots during the minima, the magnetic cycle persisted, potentially inducing abnormal changes in solar forcing (Beer et al., 1998; Foukal et al., 2011). Numerous pieces of research highlight substantial solar-forced regional climate changes during solar minima (Shindell et al., 2001; van Loon et al., 2004; Lockwood, 2010). According to Lockwood (2010), average solar activity has declined rapidly since 1985, and projections based on cosmogenic isotopes suggest an 8% probability of a return to Maunder Minimum conditions within the next 40 years. Considering the similarity in solar output radiation across multiple solar minima (Judge and Saar, 2007; Schrijver et al., 2011), an in-depth investigation of past climate changes during solar minima could significantly contribute to climate change projections for the coming decades.

Solar variability is the fundamental driving forcing for the long-term variations of EAWM, as evidenced by numerous studies (Xiao SB et al., 2006; Sagawa et al., 2014; Cho et al., 2022). Even relatively minor solar variability during GMs can significantly influence centennial-scale winter climate change in the Northern Hemisphere (Shindell et al., 2001). However, the scarcity of suitable archives and proxies for reconstructing the regional winter climate in East Asia, and for establishing connections with the long-term EAWM variability, limits our understanding of EAWM and regional climate change during the GMs. In an effort to address the knowledge gap, we have compiled records from the historical record to reconstruct the daily-resolution snowfall variations in Seoul from 1625 to 1907 CE. Centrally located in South Korea (37°33' N, 126°58' E), Seoul lies within East Asia, and is significantly affected by the EAWM, making it ideally situated for this study.

Compiling climate records from historical records is a traditional and widely accepted method for climate reconstruction, due to its accurate indication and extensive time span (e.g., Arakawa, 1956; Jung et al., 2001; Ge QS et al., 2005; Liu Y et al., 2022; Hao ZX et al., 2023). The new snowfall database provides an opportunity to explore the snowfall variations in Seoul during the two GMs (the Maunder and Dalton minima) and investigate the mechanism behind extreme solar activity on the winter climate in Northeast Asia. Meanwhile, examining these snowfall variations can assist us in understanding the evolution of solar activity during these GMs. This is an area that remains largely unexplored due to the lack of sunspot observations during the GMs, especially during the Maunder Minimum. Our research therefore provides a unique lens through which we can better comprehend these climatological phenomena.

In this paper, a brief description of the source and compilation of the snowfall dataset are provided in Section 2. We then present a dramatic reduction in the annual snowfall frequency (decadal to centennial variability) and a change in the cycle of snowfall (quasi-decadal variability) during the GMs in Section 3. Finally, in Sections 4 and 5, we discuss the possible mechanisms of solar forced snowfall variations in Seoul, before moving on to the concluding remarks.

2. Data and Method

We have compiled the daily-resolution snowfall records for Seoul spanning the period from 1625 to 1907 CE, using the Korean official historical record *Seungjeongweon Ilgi*, also named "*cheng zheng yuan ri ji* (承政院日记)" in Chinese. The record was compiled in the form of diaries documenting the activities of kings, state affairs, as well as the weather and astronomical phenomena from 1625 to 1910 CE, making it the most extensive official confidential record of the Joseon Dynasty. With the continuity and accuracy of the diary's records, the long-term weather (Lyu et al., 2023) and aurora records (Wang YQ et al., 2021) in Seoul have been compiled and used for the studies of the East Asian monsoon (Wang B et al., 2006, 2007) and the solar-terrestrial space environment (He F et al., 2021), respectively. However, the snowfall records in the diary remain largely unexplored, an oversight our research seeks to address.

Daily weather conditions were recorded at the beginning of the diary, in terms such as "snowy", "sunny", and "rainy". Any day with a recorded snowfall is defined as a snowy day in our study. Figure 1 shows an example of a qualitative snowy day record from the *Seungjeongweon Ilgi*. The illustrated record was made in the eleventh year of Emperor Tongzhi (the 10th emperor of the Qing Dynasty), in the 12th lunar month, and on the 6th day (January 4, 1873 CE), as shown in the red rectangle in Figure 1. To validate the accuracy of snowfall data, we further evaluated the continuity of weather records (Figure 2). We calculated the number of weather entries recorded annually in the diaries from 1625 to 1910, with an average of 351 entries per year (ideally, there would be daily records), indicating an almost uniformly sampled dataset. There were 10 years with annual weather records numbering fewer than 300 entries (marked as red dots in Figure 2), most notably in 1695 (a year marked by a nationwide famine and national crisis) and 1904–1905 (during the Russo–Japanese War, when the Korean Peninsula was a major theater of conflict). The Sino–Japanese War in 1894 also significantly disrupted the stability of the Joseon Dynasty. Data points with fewer than 300 annual weather entries were removed and replaced using linear interpolation to mitigate the influence of socio-political factors on data continuity. Note that the compilation does not include snowfall data for Seoul post-1907 CE, as those records have been meticulously collected, and are available on the website of the Korea Meteorological Agency (https://data.kma.go.kr/cmmn/main.do). It is worth noting that the Korean Empire fell in 1910, and the years leading up to this were marked by a turbulent political and social environment. Due to possible under-recording as a result, weather records in the *Seungjeongweon Ilgi* from this era may not be comprehensive. Users are therefore advised to exercise caution when interpreting and using these records.

Ultimately, a total of 1,479 separate snowfall records from 1625 to 1907 CE were compiled. Among these, 98% of the snowfall days fell between November and March. Accordingly, we defined two

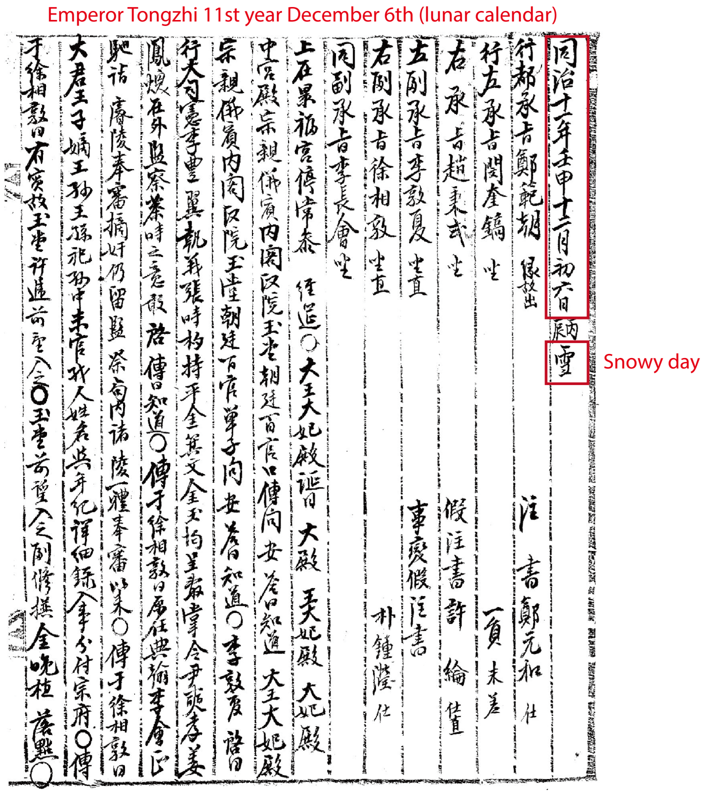

Figure 1. An example of the snowfall record in *Seungjeongweon Ilgi*. The scanned copy of this record can be accessed at the National Institute of Korean History: http://sjw.history.go.kr/id/SJW-K09120060

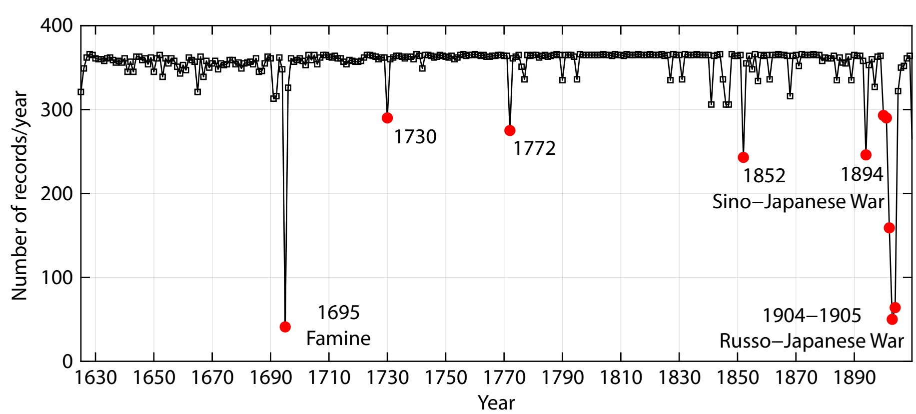

Figure 2. Annual weather records analysis in the *Seungjeongweon Ilgi* (1625–1910 CE). Ideally, the diary should contain one weather entry per day. However, due to various factors such as political turmoil and wars, some records are missing. Red circles indicate the years with fewer than 300 entries and their corresponding major historical events.

indicators, the annual snowfall frequency (ASF) and the first date of annual snowfall (FDS) each year, to describe the winter climate variations in Seoul. The ASF is calculated as the sum of snowfall days in each year; the FDS is defined as the date of the first snowfall in the winter of that particular year.

The East Asian Winter Monsoon (EAWM) is driven by the development of a cold-core high over the Siberia–Mongolia region, bringing dry and cold northwesterly air to the coastal areas of East Asia. Its intensity significantly influences winter temperatures and precipitation across the East Asian region (Wang L et al., 2012). This study selected historical temperature data and reconstructed EAWM intensity indicator near our study site (Seoul) to further verify the decadal variability of snowfall in Seoul (Figure 3). The temperature reconstructions in Japan were based on cherry blossom phenological data from Tokyo (Figure 3, R1) and Kyoto (Figure 3, R2), reflecting the average temperature changes in March for the region. For northeastern China, temperature data were reconstructed using tree-ring width records of Korean pine from the Changbai Mountain, representing the average temperatures from February to April (Figure 3, R3). The wind speed of the EAWM was reconstructed based on cross-front transport characteristics of sediments in the North Yellow Sea (Figure 3, R4). The resolution of the original temperature data is annual. The resolu-

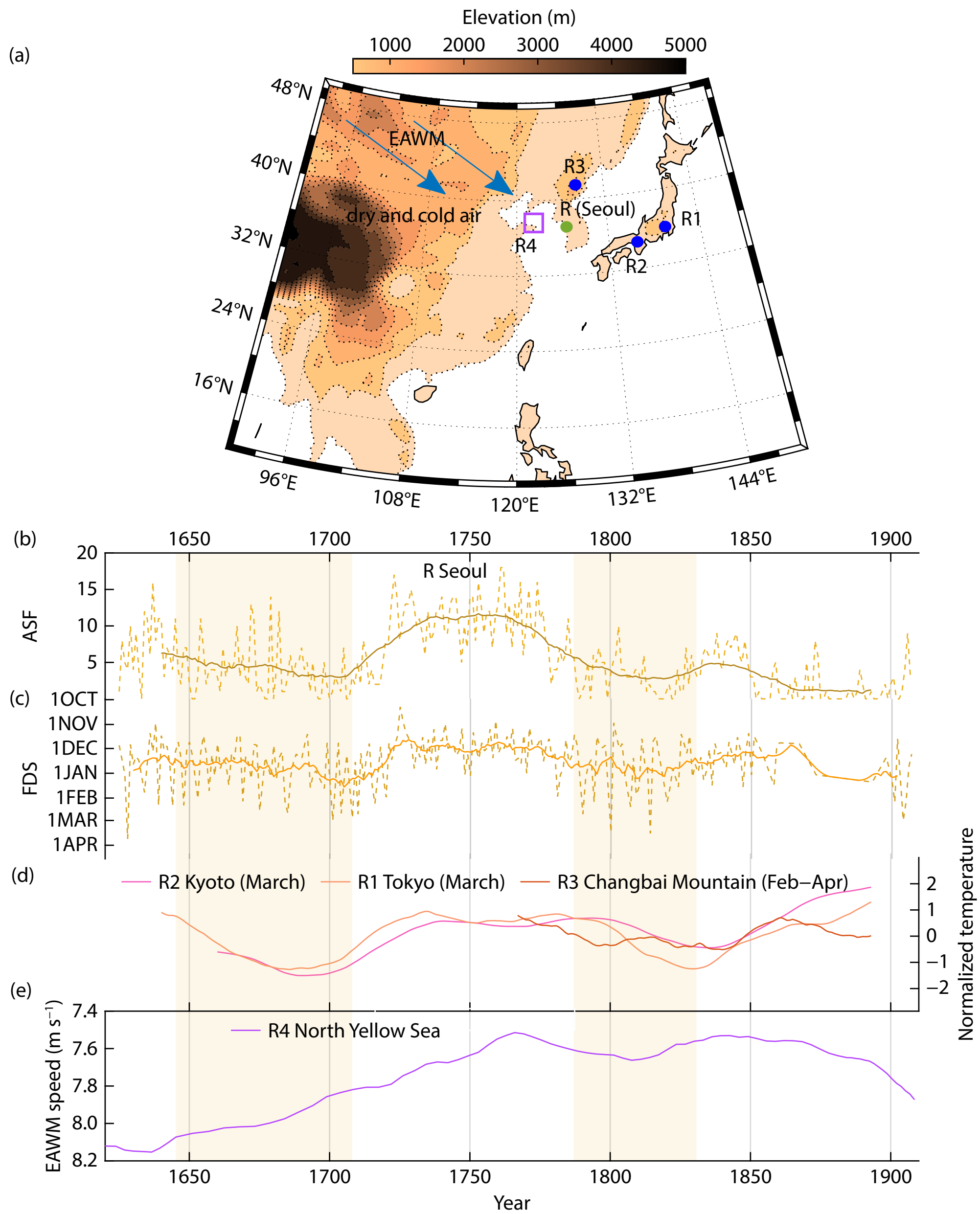

Figure 3. Comparison of annual snowfall frequency (ASF) reconstruction in Seoul and other climate indicators across East Asia over a decadal to centennial scale. (a) Map showing data locations in this study. Shading indicates different altitudes, with darker shades representing higher elevations and lighter shades representing lower ones. (b) The reconstructed FDS in Seoul from 1625 to 1907 CE. The bolded lines show the 30-year moving average of the original annual data. (c) The reconstructed ASF in Seoul from 1625 to 1907 CE. The bolded lines show the 30-year moving average of the original annual data. 1OCT means October 1st. (d) The mean March temperatures of Kyoto and Tokyo, Japan, as reconstructed by Aono and Kazui (2008, purple line) and Aono (2015, pink line). The red line shows the tree ring-based February–April temperature reconstruction for Changbai Mountain in Northeast China (Zhu HF et al., 2009). The temperatures have been normalized to a standard scale. The bolded lines show the 30-year moving average of the original annual data. (e) The EAWM speed reconstructed from the cross-front transport characteristics of sediments in the North Yellow Sea, note: the *y*-axis is inverted (Shi Y et al., 2023).

tion of the EAWM index is approximately three years. In this study, linear interpolation was used to refine its temporal resolution to an annual scale. The results demonstrate that prior to 1850 (i.e., the pre-industrial period), Seoul's ASF exhibited a significant negative correlation with the EAWM (annual correlation coefficient: −0.41, $p < 0.001$), and a significant positive correlation with temperature (annual correlation coefficients with the temperatures: 0.48 for Tokyo, 0.49 for Kyoto, and 0.40 for Changbai Mountain, with all $p < 0.001$). Two periods of notable ASF decline (1645–1715 CE and 1790–1830 CE) coincided with lower temperatures in surrounding regions and stronger EAWM phases. This suggests that under natural climate conditions, an increase in temperature typically enhances the evaporation and transport capacity of atmospheric water vapor, thereby providing more abundant moisture for snowfall. When winter temperatures approach the critical threshold for snowfall, weaker dry EAWM combined with higher temperature may instead promote the occurrence of snowfall.

This study employs the wavelet analysis method to investigate the periodic characteristics of snowfall. Unlike traditional Fourier transform, wavelet analysis can simultaneously capture the variation features of signals in both the time and frequency domains, making it particularly suitable for analyzing non-stationary signals (Mallat, 1989). By convolving the signal with a set of wavelet functions at different scales and positions, wavelet analysis extracts the energy distribution of the signal across various time scales, thereby revealing its periodic characteristics and time-localized properties. The snowfall data used in this study is an annual continuous series, thus, the continuous wavelet transform is applied to analyze the periodic features within the data (Aguiar-Conraria and Soares, 2014).

3. Results

3.1 Reduced Snowfall during the GMs

Over the past 400 years, solar activity had experienced two famous GMs, namely the Maunder Minimum during 1645–1715 CE (Eddy, 1976) and the Dalton Minimum from 1790 to 1830 CE (Wagner and Zorita, 2005). These periods are distinctly marked by variations in the Group Sunspot Number (GSN) and Total Solar Irradiance (TSI) reconstructions (Figure 4c). The ASF index shows a clear shift during these GMs (Figure 4a). Notably, there is a prolonged period of exceptionally low annual snowfall frequency leading up to 1715 CE, lasting for over half a century during the Maunder Minimum, followed by a rapid increase after 1715 CE. The annual snowfall frequency then begins to decline gradually in the middle of the 18th century, persisting at a low level during the Dalton Minimum. The variations of the FDS index are in good agreement with those of ASF index, which is manifested as the significant delay of the first snow date during both the Maunder and Dalton minima (Figure 4b). Within these two GMs, the average date of the annual first snowfall started about 10 days later, and the average annual snowfall frequency decreased by half, compared to the periods outside of these solar minima.

Colder winters in the Northern Hemisphere during the Maunder Minimum have been widely studied (Luterbacher et al., 2001). While lower temperatures may typically mean more winter snowfall, our reconstruction suggests that snowfall is less likely to occur in Seoul during the GMs, as evidenced by the reduced snowfall frequency and the delayed onset of first snowfall each winter. Here, we emphasize that temperature and water vapor jointly regulate the process of winter snowfall. When winter temperatures remain consistently below 0°C, the dominant factor influencing the intensity of snowfall may no longer be temperature, but rather water vapor. Therefore, we speculate that the weak snowfall in Seoul may be mainly attributable to a lack of water vapor content in the atmosphere. The decrease in solar forcing could weaken the Hadley circulation (Haigh, 1996, 2003), thereby reducing the amount of water vapor delivered to Seoul. At the same time, the increased snowfall over the Siberian high region during these colder periods would intensify the EAWM (Jhun and Lee, 2004), further inhibiting the arrival of water vapor from the south to Seoul (Wang and He, 2013).

3.2 The Variations in Snowfall Cycle During the GMs

The most pronounced quasi-periodic variation of solar activity is

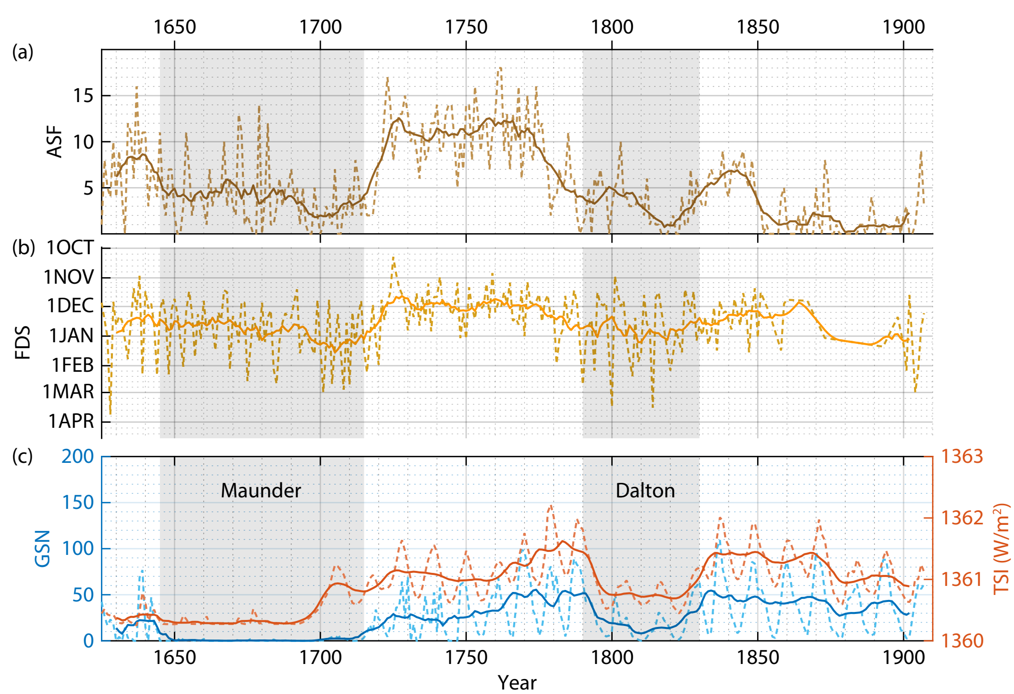

Figure 4. Comparison of the snowfall records with the reconstructed solar activity indices. The dashed lines represent the raw annual resolution data, while the solid lines denote an 11-year running mean of the raw data. (a) The variations of the annual snowfall frequency (ASF). (b) The variations between the first dates of snowfall in each year (FDS). For instance, 1OCT means October 1st. (c) The variations of the Group Sunspot Number (GSN) from Hoyt et al. (1998), and the Total Solar Irradiance (TSI) reconstruction from Kopp et al. (2016).

the Schwabe cycle (Usoskin, 2017), fluctuating between 9 and 14 years in duration with an averaged cycle of ~11 years. Although climate simulations indicated a minor climatic response to the decadal solar cycle (Wigley and Raper, 1990), subsequent modeling studies have found both resonant responses and positive feedbacks in the ocean–atmosphere system that may amplify the response to solar irradiance variations (White and Liu, 2008; Meehl et al., 2009). In this section, we focus on the variability of snowfall at the solar cycle scale, to better understand the snowfall responses to solar activity during the GMs.

To study the snowfall variations at the solar cycle scale, we band-pass filtered the annual snowfall frequency, extracting the signal within the 7–16 years period (Figure 5a), and then performed the normalized wavelet periodicity analysis. Results suggest a clear transition in cycles. During periods outside the GMs, the cycle length is ~11 years, while it shortens to 8–9 years during the GMs before the industrial revolution. As shown in Figure 5b, during the Maunder Minimum (1645–1715 CE), the snowfall cycle was predominantly 8–9 years in duration. From 1715 onwards, the snowfall cycle gradually lengthened to ~11 years. However, with the beginning of the Dalton Minimum (1790–1830 CE), the snowfall cycle gradually contracted back to the 8–9 year range, persisting in this state until 1830 CE.

The existence of a Schwabe cycle in the Sun's energy output, with a period of approximately 11 years, is well-established. The snowfall variations exhibit a similar ~11-year cycle, indicating that solar activity variations in the Schwabe cycle potentially have influence on snowfall patterns. In addition to the dominant 11-year solar activity variations, a weak ~8-year cyclic variation has been identified in solar activity proxies, such as the sunspot numbers (Krivova and Solanki, 2002; Zhu FR and Jia HY, 2018), $F_{10.7}$ flux (Roy et al., 2019) and aurora (Yan LM et al., 2023), raising the possibility that the ~8-year cycle observed in snowfall may also correspond to changes in solar activity. The alignment of the ~8-year snowfall cycle with periods of low solar activity suggests its potential as an indicator of reduced solar activity. However, understanding the underlying reasons for the transition of snowfall variations from a ~11-year cycle to an ~8-year cycle necessitates further investigation, which lies beyond the scope of the present study.

4. Discussion

This study on the historical snowfall patterns in Seoul reveals that under natural climate conditions, periods of significantly weakened solar activity were accompanied by decreases in temperature and snowfall. However, since the Second Industrial Revolution, with the profound disturbances caused by human activities to the climate system, the relationship between snowfall and temperature in Seoul has gradually reversed, showing a negative correlation — higher temperature is now associated with decreased snowfall (Figure 6a, b). The correlation coefficient between annual snowfall frequency and winter mean temperature (WMT) in Seoul is −0.5 ($p < 0.001$). This shift reflects the complex impacts of global warming on regional climate systems. On the one hand, higher temperatures limit the conditions for winter snowfall formation, particularly in low-altitude areas where temperatures may exceed the threshold required for snowfall, causing more water vapor to fall as rain rather than snow. On the other hand, rising temperatures may alter the pathways and intensity of atmospheric moisture transport, such as enhancing warm and moist airflows from the

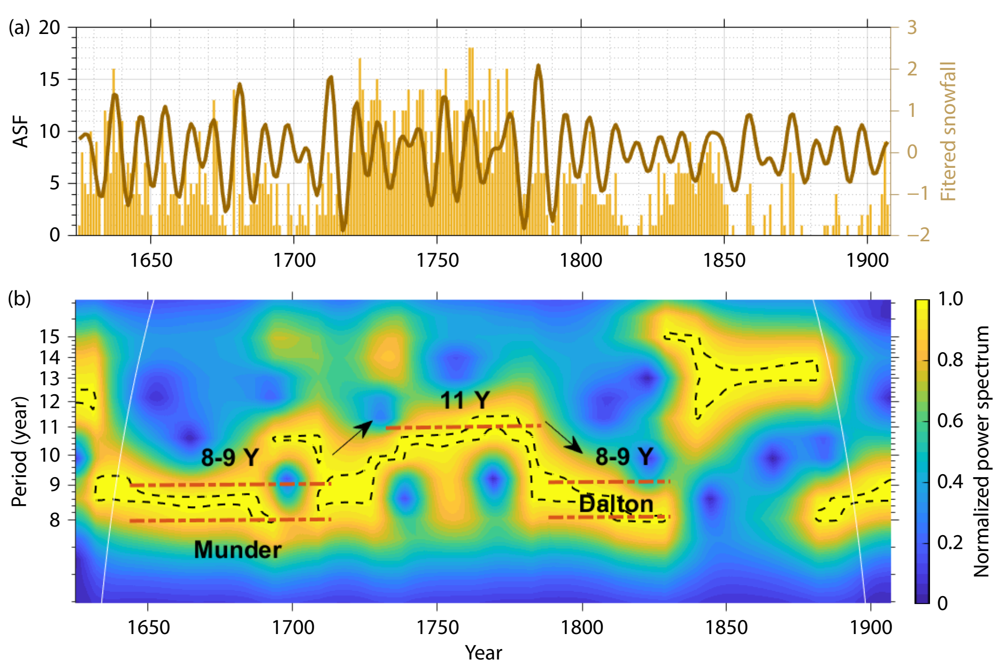

Figure 5. Continuous Wavelet Transform (CWT) of the reconstructed snowfall. (a) The variations of annual snowfall frequency depicted both before and after filtering with a bar graph and a curve, respectively. (b) The normalized wavelet periodicity analysis of the filtered annual snowfall frequency. The spectra were normalized for each respective year within the period interval of 7–16 years. The black dashed line corresponds to the normalized spectral value of 0.98. The white line represents the cone of influence, a region where the results of the wavelet transform may be distorted due to edge effects..

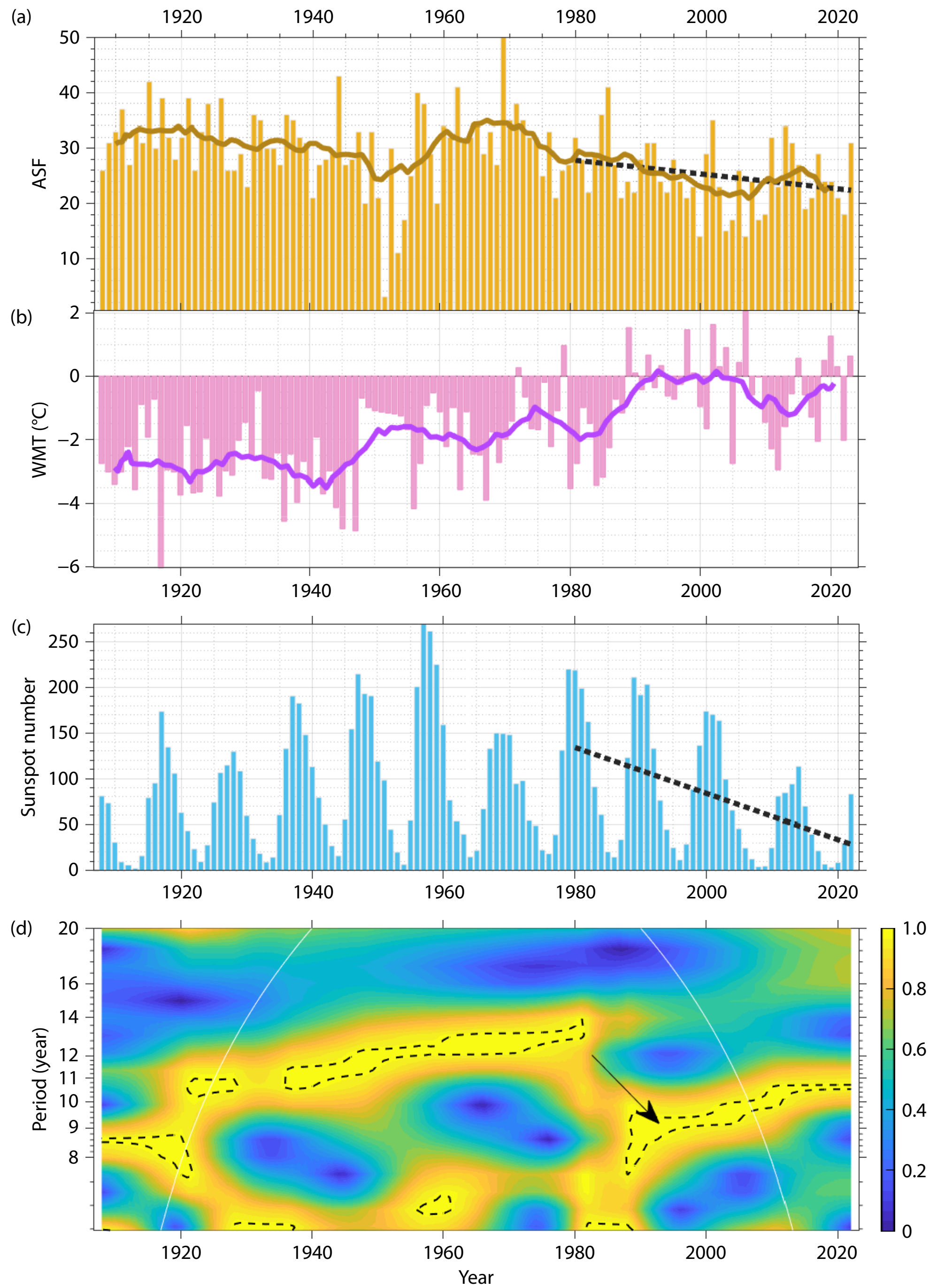

Figure 6. Comparison of the instrumental annual snowfall frequency in Seoul with the winter mean temperature and sunspot variations from 1908 to 2022 CE. (a) The variations of annual snowfall frequency in Seoul, with data sourced from the website of the Korea Meteorological Agency (https://data.kma.go.kr/cmmn/main.do). The curve represents the 10-year sliding average of ASF. The black dotted line represents a first-order linear fitting trend for the annual snowfall frequency from 1980 to 2022 CE, suggesting a decline in Seoul since 1980 CE. (b) The variations of annual winter mean temperature (WMT) in Seoul. The curve represents the 10-year moving average of WMT. (c) The variations of sunspot number. The black dotted line represents a first-order linear fit, indicating that the solar activity has been declining since the 21st solar cycle. (d) The normalized wavelet periodicity analysis of the annual snowfall frequency. The spectra were normalized for each respective year during the period interval of 7–16 years. The black dashed line corresponds to the normalized spectral value of 0.98. The white line denotes the cone of the influence due to the edge effect of the wavelet transform.

ocean, which further influences snowfall patterns.

Today's solar activity exhibits peculiar characteristics. The magnetic activity of the sun was notably weak during the years 2006–2009 CE, with sunspot numbers reaching the lowest values in approximately 100 years. By the end of the 23rd solar cycle, the annual mean of the open solar magnetic flux (deduced from geomagnetic activity) had fallen to a level last seen in 1924 CE

(Lockwood et al., 2009). The 24th solar cycle, which continues to diminish, is also marked by an unusual field reversal pattern of the Sun (Janardhan et al., 2018). The recent prolonged solar minimum and the subsequent weak 24th solar cycle have led to suggestions that we might be the verge of the next grand solar minimum, which could affect future climate (Meehl et al., 2013; Ineson et al., 2015). In our analysis of the historical snowfall records, we observed that the snowfall frequency in Seoul was remarkably low during the Maunder and Dalton Minima. If this pattern continues, we may begin to observe indications of a shift toward the next period of reduced solar activity reflected in contemporary snowfall patterns in Seoul. Figure 6 illustrates the variations in snowfall in Seoul alongside sunspot numbers from 1908 to 2022 CE. Since the 1980s, there has been a noticeable decline in snowfall frequency in Seoul, which aligns with the reduction in solar activity (Figure 6a, b). Interestingly, as solar activity began to wane during the 21st solar cycle in the 1980s, the snowfall cycle in Seoul shortened to 8–9 years (Figure 6c), mirroring patterns observed during the Maunder and Dalton Minima. However, this shortened snowfall cycle was short-lived, gradually transitioning back to the 11-year cycle after Solar Cycle 23. This return to the longer cycle may suggest a solar minimum that failed to fully develop.

This study delve into the potential influence of solar activity on climate changes, involving three specific processes. The first mechanism (top–down mechanism) involves variations in the solar cycle that can induce changes in the incident radiative flux at the top of the Earth's atmosphere. These changes then affect the radiative heating effect of greenhouse gases (including ozone, water vapor, and so on) within the stratosphere. As a result, an abnormal temperature gradient is generated within the stratosphere, which influences the intensity of stratospheric circulation (e.g., Matthes et al., 2017). Previous studies have illustrated that these abnormal changes from stratospheric circulation can propagate downwards, instigating alterations in tropospheric weather and climate at mid-to-high latitudes (Haynes et al., 1991; Baldwin and Dunkerton., 2001; Li DL et al., 2019). Recently, this anomalous stratospheric circulation caused by the radiation process has been found to affect even tropical climates (Xie F et al., 2016).

The second mechanism (bottom-up mechanism) involves the direct effect of the TSI on the ocean's surface, which could be amplified by a feedback mechanism involving water vapor transport from the tropical Pacific (Meehl et al., 2009; Huo WJ et al., 2023). This hypothesis aligns with observed cooler conditions in the mid-latitudes and drier tropics, indicating a contraction of the Hadley cells (van Geel et al., 1999). Moreover, fluctuations in the TSI can lead to variations in the temperature of the oceanic mixed layer. This, in turn, modulates the interaction between the ocean and the atmosphere, specifically affecting systems such as the Walker circulation, exemplified in phenomena like the El Niño-Southern Oscillation (Gray et al., 2010).

The third mechanism proposed involves a cosmic ray–cloud effect. Variations in cosmic ray flux, linked to variations in solar wind, may trigger climate change through amplification of changing solar radiation. Lower levels of solar activity result in greater penetration of both galactic and solar cosmic ray fluxes into the stratosphere and troposphere, initiating physical and chemical reactions, such as a change in low cloud cover. During the 11-year solar cycle, changes in galactic cosmic ray fluxes could reach about 10% relative to the flux during solar minimum on the Earth's surface and about 50% in the stratosphere. More pronounced changes in cosmic ray intensity could occur during the GMs, similarly to the Maunder Minimum (van Geel et al., 1999; Carslaw et al., 2002; Kirkby, 2007). Evidence suggests that increased GCR flux is associated with a southward shift of the Intertropical Convergence Zone (ITCZ) (Newton et al., 2006). Considering that the ITCZ is the primary source of water vapor for the upper troposphere in the tropics and sub-tropics, a southward shift of the ITCZ during the DM could reduce the amount of water vapor traveling northward.

Meanwhile, another possible climate driver during the Maunder Minimum is highlighted here: the geomagnetic anomaly in the Western Pacific (WPA). A recent study reported a notable low-intensity geomagnetic anomaly in the northwestern Pacific Ocean during the seventeenth to eighteenth centuries, with a significant number of auroras observed in Seoul, possibly triggered by this same anomaly (He F et al., 2021). During the Maunder Minimum, the increased incidence of cosmic rays on Earth, coupled with the WPA potentially providing an optimal channel for cosmic rays, could have further amplified the cosmic ray–cloud effect and the influence of solar forcing on climate.

The synergistic interplay between various mechanisms could potentially amplify the minor effects of solar activity, leading to more significant impacts on climate (Meehl et al., 2009; Zhao L et al., 2017). This effect becomes especially prominent in the marginal zones of certain localized climate systems, where solar signals may be more readily discernible. These regions, where the signals of external factors are particularly pronounced, provide clearer windows into their effects on localized climate systems (Zhao L and Wang JS, 2014).

5. Conclusions

The limited availability of long-term winter climate proxies has left the effects of solar variability on Northeast Asia's winter climate, particularly during grand solar minima (GMs), largely uncertain. Understanding these potential solar influences is essential for enhancing the accuracy of future climate projections. In this study, we reconstructed daily snowfall records in Seoul spanning from 1625 to 1907 CE using the Korean official historical document, *Seungjeongwon Ilgi*. This reconstruction encompasses both the Maunder Minimum (1645–1715 CE) and the Dalton Minimum (1790–1830 CE), offering a dataset characterized by its extensive temporal coverage, high resolution, and clear climatological significance independent of other natural factors.

Our analysis reveals a notable weakening of winter snowfall in Seoul during the Maunder and Dalton Minima. Specifically, the onset of annual snowfall was delayed by approximately 10 days, and the average annual snowfall frequency was reduced by half compared to non-GM periods. Furthermore, the typical ~11-year snowfall cycle is replaced by an 8- to 9-year cycle during these grand minima. Remarkably, a similar pattern has reemerged in recent decades: since the 21st solar cycle in the 1980s, decreasing solar activity has coincided with a shortening of Seoul's snowfall cycle to 8–9 years. Based on these historical patterns, we hypothesize that such cyclical changes may serve as climatic indicators of impending shifts in long-term solar activity, potentially signaling the onset of the next period of significantly low solar activity.

We attribute the observed reduction in snowfall to diminished moisture transport to Seoul, resulting from alterations in the East Asian Winter Monsoon (EAWM) and regional circulation systems during the grand solar minima. The influence of solar activity on Seoul's winter climate appears to operate through three primary mechanisms: the top-down mechanism, the bottom-up mechanism, and the cosmic ray–cloud effect. Additionally, the recently proposed low-intensity geomagnetic Wolf Pine Anomaly (WPA) during the Maunder Minimum may amplify the cosmic ray–cloud interactions, further modulating winter climate conditions.

Acknowledgments

We thank Ziniu Xiao, Liang Zhao and Fei Xie for help with the discussion. This work is supported by the National Natural Science Foundation of China (Grant No. 42388101), the National Natural Science Foundation of China (42241106) and CAS Youth Interdisciplinary Team (JCTD-2021-05).

Open Research

The Seoul snowfall data can be accessed at the World Data Center (WDC) for Geophysics, Beijing (Wang, 2022) via the following link: https://doi.org/10.12197/2022GA001.

References

Aguiar-Conraria, L., and Soares, M. J. (2014). The continuous wavelet transform: Moving beyond UNI-and bivariate analysis. *J. Econom. Surv.*, *28*(2), 344–375. https://doi.org/10.1111/joes.12012

Aono, Y., and Kazui, K. (2008). Phenological data series of cherry tree flowering in Kyoto, Japan, and its application to reconstruction of springtime temperatures since the 9th century. *Int. J. Climatol.*, *28*(7), 905–914. https://doi.org/10.1002/joc.1594

Aono, Y. (2015). Cherry blossom phenological data since the seventeenth century for Edo (Tokyo), Japan, and their application to estimation of March temperatures. *Int. J. Biometeor.*, *59*(4), 427–434. https://doi.org/10.1007/s00484-014-0854-0

Arakawa, H. (1956). On the secular variation of annual totals of rainfall at Seoul from 1770 to 1944. *Arch Met. Geoph. Biokl. Ser. B*, *7*(2), 205–211. https://doi.org/10.1007/BF02243323

Baldwin, M. P., and Dunkerton, T. J. (2001). Stratospheric harbingers of anomalous weather regimes. *Science*, *294*(5542), 581–584. https://doi.org/10.1126/science.1063315

Beer, J., Tobias, S., and Weiss, N. (1998). An active sun throughout the maunder minimum. *Solar Phys.*, *181*(1), 237–249. https://doi.org/10.1023/A:1005026001784

Braun, H., Christl, M., Rahmstorf, S., Ganopolski, A., Mangini, A., Kubatzki, C., Roth, K., and Kromer, B. (2005). Possible solar origin of the 1,470-year glacial climate cycle demonstrated in a coupled model. *Nature*, *438*(7065), 208–211. https://doi.org/10.1038/nature04121

Carslaw, K. S., Harrison, R. G., and Kirkby, J. (2002). Cosmic rays, clouds, and climate. *Science*, *298*(5599), 1732–1737. https://doi.org/10.1126/science.1076964

Cho, A., Lim, J., Kim, Y., and Ahn, U. S. (2022). Variability of East Asian winter monsoon during middle–Late Holocene: A study based on a crater lake on Jeju Island, South Korea. *Palaeogeogr. Palaeoclimatol. Palaeoecol.*, *603*, 111193. https://doi.org/10.1016/j.palaeo.2022.111193

Eddy, J. A. (1976). The maunder minimum: The reign of Louis XIV appears to have been a time of real anomaly in the behavior of the sun. *Science*, *192*(4245), 1189–1202. https://doi.org/10.1126/science.192.4245.1189

Feng, S. N., Liu, X. Q., and Mao, X. (2023). Vegetation dynamics in arid central Asia over the past two millennia linked to NAO variability and solar forcing. *Quat. Sci. Rev.*, *310*, 108134. https://doi.org/10.1016/j.quascirev.2023.108134

Foukal, P., Ortiz, A., and Schnerr, R. (2011). Dimming of the 17th century sun. *Astrophys. J. Lett.*, *733*(2), L38. https://doi.org/10.1088/2041-8205/733/2/l38

Ge, Q. S., Zheng, J. Y., Hao, Z. X., Zhang, P. Y., and Wang, W. C. (2005). Reconstruction of historical climate in china: High-resolution precipitation data from Qing dynasty archives. *Bull. Am. Meteor. Soc.*, *86*(5), 671–680. https://doi.org/10.1175/BAMS-86-5-671

Gray, L. J., Beer, J., Geller, M., Haigh, J. D., Lockwood, M., Matthes, K., Cubasch, U., Fleitmann, D., Harrison, G., … White, W. (2010). Solar influences on climate. *Rev. Geophys.*, *48*(4), RG4001. https://doi.org/10.1029/2009RG000282

Haigh, J. D. (1996). The impact of solar variability on climate. *Science*, *272*(5264), 981–984. https://doi.org/10.1126/science.272.5264.981

Haigh, J. D. (2003). The effects of solar variability on the Earth's climate. *Philos. Trans. Roy. Soc. A: Math., Phys. Eng. Sci.*, *361*(1802), 95–111. https://doi.org/10.1098/rsta.2002.1111

Hao, Z. X., Zheng, J. Y., Ge, Q. S., and Bai, M. X. (2023). A 2.5°×2.5° gridded drought/flood grades dataset for eastern China during the last millennium. *Sci. Data*, *10*(1), 202. https://doi.org/10.1038/s41597-023-02110-5

Haynes, P. H., McIntyre, M. E., Shepherd, T. G., Marks, C. J., and Shine, K. P. (1991). On the "downward control" of extratropical diabatic circulations by eddy-induced mean zonal forces. *J. Atmos. Sci.*, *48*(4), 651–678. https://doi.org/10.1175/1520-0469(1991)048<0651:OTCOED>2.0.CO;2

He, F., Wei, Y., Maffei, S., Livermore, P. W., Davies, C. J., Mound, J., Xu, K. H., Cai, S. H., and Zhu, R. X. (2021). Equatorial auroral records reveal dynamics of the paleo-west pacific geomagnetic anomaly. *Proc. Nat. Acad. Sci. USA*, *118*(20), e2026080118. https://doi.org/10.1073/pnas.2026080118

Hoyt, D. V., and Schatten, K. H. (1998). Group sunspot numbers: A new solar activity reconstruction. *Sol. Phys.*, *179*(1), 189–219. https://doi.org/10.1023/A:1005007527816

Huo, W. J., Xiao, Z. N., and Zhao, L. (2023). Phase-locked impact of the 11-year solar cycle on tropical pacific decadal variability. *J. Climate*, *36*(2), 421–439. https://doi.org/10.1175/JCLI-D-21-0595.1

Ineson, S., Maycock, A. C., Gray, L. J., Scaife, A. A., Dunstone, N. J., Harder, J. W., Knight, J. R., Lockwood, M., Manners, J. C., and Wood, R. A. (2015). Regional climate impacts of a possible future grand solar minimum. *Nat. Commun.*, *6*(1), 7535. https://doi.org/10.1038/ncomms8535

Janardhan, P., Fujiki, K., Ingale, M., Bisoi, S. K., and Rout, D. (2018). Solar cycle 24: An unusual polar field reversal. *Astron. Astrophys.*, *618*(10), A148. https://doi.org/10.1051/0004-6361/201832981

Jhun, J. G., and Lee, E. J. (2004). A new East Asian winter monsoon index and associated characteristics of the winter monsoon. *J. Climate*, *17*(4), 711–726. https://doi.org/10.1175/1520-0442(2004)017<0711:ANEAWM>2.0.CO;2

Jin, C., Wang, B., Liu, J., Ning, L., and Yan, M. (2019). Decadal variability of northern Asian winter monsoon shaped by the 11-year solar cycle. *Climate Dyn.*, *53*(11), 6559–6568. https://doi.org/10.1007/s00382-019-04945-4

Judge, P. G., and Saar, S. H. (2007). The outer solar atmosphere during the maunder minimum: A stellar perspective. *Am. Astrophys. J.*, *663*(1), 643. https://doi.org/10.1086/513004

Jung, H. S., Lim, G. H., and Oh, J. H. (2001). Interpretation of the transient variations in the time series of precipitation amounts in Seoul, Korea. Part I: Diurnal variation. *J. Climate*, *14*(13), 2989–3004. https://doi.org/10.1175/1520-0442(2001)014<2989:IOTTVI>2.0.CO;2

Kirkby, J. (2007). Cosmic rays and climate. *Surv. Geophys.*, *28*(5), 333–375. https://doi.org/10.1007/s10712-008-9030-6

Kopp, G., Krivova, N., Wu, C. J., and Lean, J. (2016). The impact of the revised sunspot record on solar irradiance reconstructions. *Sol. Phys.*, *291*(9), 2951–2965. https://doi.org/10.1007/s11207-016-0853-x

Krivova, N. A., and Solanki, S. K. (2002). The 1.3-year and 156-day periodicities in sunspot data: wavelet analysis suggests a common origin. *Astron. Astrophys.*, *394*(2), 701–706. https://doi.org/10.1051/0004-6361:20021063

Lean, J. L. (2010). Cycles and trends in solar irradiance and climate. *Wiley Interdiscip. Rev. Climate Change*, *1*(1), 111–122. https://doi.org/10.1002/wcc.18

Li, D. L., Xiao, Z. N., and Zhao, L. (2019). Preferred solar signal and its transfer in the Asian–Pacific subtropical jet region. *Climate Dyn.*, *52*(9-10), 5173–5187, https://doi.org/10.1007/s00382-018-4443-5

Liu, Y., Zheng, J. Y., Hao, Z. X., and Ge, Q. S. (2022). A dataset of standard precipitation index reconstructed from multi-proxies over Asia for the past 300 years. *Earth Syst. Sci. Data*, *14*(12), 5717–5735. https://doi.org/10.5194/essd-14-5717-2022

Lockwood, M., Rouillard, A. P., and Finch, I. D. (2009). The rise and fall of open solar flux during the current grand solar maximum. *Astrophys. J.*, *700*(2), 937. https://doi.org/10.1088/0004-637X/700/2/937

Lockwood, M. (2010). Solar change and climate: an update in the light of the current exceptional solar minimum. *Proc. Roy. Soc. A: Math., Phys. Eng. Sci.*, *466*(2114), 303–329. https://doi.org/10.1098/rspa.2009.0519

Luterbacher, J., Rickli, R., Xoplaki, E., Tinguely, C., Beck, C., Pfister, C., and Wanner, H. (2001). The late Maunder minimum (1675–1715) — a key period forstudying decadal scale climatic change in Europe. *Climatic Change*, *49*(4), 441–462. https://doi.org/10.1023/A:1010667524422

Lyu, Z., Ichikawa, K., Cheng, Y. C., Hayakawa, H., and Kawamoto, Y. (2023). Digitization of weather records of *Seungjeongwon Ilgi*: A historical weather dynamics dataset of the Korean Peninsula in 1623–1910. *Geosci. Data J.*, *11*(4), 504–513. https://doi.org/10.1002/gdj3.227

Ma, H. D., Chen, H. S., Lai, A. W., Li, X., Wang, R. L., and Gao, C. J. (2019). Robust solar signature in late winter precipitation over southern China. *Geophys. Res. Lett.*, *46*(16), 9940–9948. https://doi.org/10.1029/2019GL084083

Mallat, S. G. (1989). A theory for multiresolution signal decomposition: the wavelet representation. *IEEE Trans. Patt. Anal. Mach. Intell.*, *11*(7), 674–693. https://doi.org/10.1109/34.192463

Matthes, K., Funke, B., Andersson, M. E., Barnard, L., Beer, J., Charbonneau, P., Clilverd, M. A., De Wit, T. D., Haberreiter, M., …Versick, S. (2017). Solar forcing for CMIP6 (v3.2). *Geosci. Model Dev.*, *10*(6), 2247–2302. https://doi.org/10.5194/gmd-10-2247-2017

Meehl, G. A., Arblaster, J. M., Matthes, K., Sassi, F., and van Loon, H. (2009). Amplifying the pacific climate system response to a small 11-year solar cycle forcing. *Science*, *325*(5944), 1114–1118. https://doi.org/10.1126/science.1172872

Meehl, G. A., Arblaster, J. M., and Marsh, D. R. (2013). Could a future "Grand Solar Minimum" like the Maunder Minimum stop global warming?. *Geophys. Res. Lett.*, *40*(9), 1789–1793. https://doi.org/10.1002/grl.50361

Muñoz-Jaramillo, A., and Vaquero, J. M. (2019). Visualization of the challenges and limitations of the long-term sunspot number record. *Nat. Astron.*, *3*(3), 205–211. https://doi.org/10.1038/s41550-018-0638-2

Neff, U., Burns, S. J., Mangini, A., Mudelsee, M., Fleitmann, D., and Matter, A. (2001). Strong coherence between solar variability and the monsoon in Oman between 9 and 6 kyr ago. *Nature*, *411*(6835), 290–293. https://doi.org/10.1038/35077048

Newton, A., Thunell, R., and Stott, L. (2006). Climate and hydrographic variability in the Indo-Pacific Warm Pool during the last millennium. *Geophys. Res. Lett.*, *33*(19), L19710. https://doi.org/10.1029/2006GL027234

Roy, S., Prasad, A., Panja, S. C., Ghosh, K., and Patra, S. N. (2019). A search for periodicities in *F*10.7 solar radio flux data. *Sol. Syst. Res.*, *53*(3), 224–232. https://doi.org/10.1134/S0038094619030031

Sagawa, T., Kuwae, M., Tsuruoka, K., Nakamura, Y., Ikehara, M., and Murayama, M. (2014). Solar forcing of centennial-scale East Asian winter monsoon variability in the mid- to late Holocene. *Earth Planet. Sci. Lett.*, *395*, 124–135. https://doi.org/10.1016/j.epsl.2014.03.043

Schrijver, C. J., Livingston, W. C., Woods, T. N., and Mewaldt, R. A. (2011). The minimal solar activity in 2008–2009 and its implications for long-term climate modeling. *Geophys. Res. Lett.*, *38*(6), L06701. https://doi.org/10.1029/2011GL046658

Shi, Y., Xu, X. M., Yang, G., Du, J. B, Lü, J. X., Zhang, S., Liu, S. J., Liu, T., Zhang, Z. Y., and Gao, J. H. (2023). High-resolution records of millennial-scale east Asian winter monsoon in the shelf sea of eastern China. *Geophys. Res. Lett.*, *50*(7), e2022GL102302. https://doi.org/10.1029/2022GL102302

Shindell, D. T., Schmidt, G. A., Mann, M. E., Rind, D., and Waple, A. (2001). Solar forcing of regional climate change during the maunder minimum. *Science*, *294*(5549), 2149–2152. https://doi.org/10.1126/science.1064363

Siscoe, G. L. (1978). Solar–terrestrial influences on weather and climate. *Nature*, *276*(5686), 348–352. https://doi.org/10.1038/276348a0

Solanki, S. K., Krivova, N. A., and Haigh, J. D. (2013). Solar irradiance variability and climate. *Ann. Rev. Astron. Astrophys.*, *51*, 311–351. https://doi.org/10.1146/annurev-astro-082812-141007

Usoskin, I. G. (2017). A history of solar activity over millennia. *Living Rev. Sol. Phys.*, *14*(1), 3. https://doi.org/10.1007/s41116-017-0006-9

van Geel, B., Raspopov, O. M., Renssen, H., van der Plicht, J., Dergachev, V. A., and Meijer, H. A. J. (1999). The role of solar forcing upon climate change. *Quat. Sci. Rev.*, *18*(3), 331–338. https://doi.org/10.1016/S0277-3791(98)00088-2

van Loon, H., Meehl, G. A., and Arblaster, J. M. (2004). A decadal solar effect in the tropics in July–August. *J. Atmos. Solar-Terr. Phys.*, *66*(18), 1767–1778. https://doi.org/10.1016/j.jastp.2004.06.003

Wagner, S., and Zorita, E. (2005). The influence of volcanic, solar and CO_2 forcing on the temperatures in the Dalton Minimum (1790–1830): a model study. *Climate Dyn.*, *25*(2), 205–218. https://doi.org/10.1007/s00382-005-0029-0

Wang, B., Ding, Q. H., and Jhun, J. G. (2006). Trends in Seoul (1778-2004) summer precipitation. *Geophys. Res. Lett.*, *33*(15), L15803. https://doi.org/10.1029/2006GL026418

Wang, B., Jhun, J. G., and Moon, B. K. (2007). Variability and singularity of seoul, south korea, rainy season (1778–2004). *J. Climate*, *20*(11), 2572–2580. https://doi.org/10.1175/JCLI4123.1

Wang, H. J., and He, S. P. (2013). The increase of snowfall in Northeast China after the mid-1980s. *Chin. Sci. Bull.*, *58*(12), 1350–1354. https://doi.org/10.1007/s11434-012-5508-1

Wang, L., Li, J. J., Lu, H. Y., Gu, Z. Y., Rioual, P., Hao, Q. Z., Mackay, A. W., Jiang, W. Y., Cai, B. G., and Chu, G. Q. (2012). The East Asian winter monsoon over the last 15,000 years: its links to high-latitudes and tropical climate systems and complex correlation to the summer monsoon. *Quat. Sci. Rev.*, *32*, 131–142. https://doi.org/10.1016/j.quascirev.2011.11.003

Wang, Y. Q., Chen, S., Xu, K. H., Yan, L. M., Yue, X. N., He, F., and Wei, Y. (2021). Ancient auroral records compiled from Korean historical books. *J. Geophys. Res.: Space Phys.*, *126*(1), e2020JA028763. https://doi.org/10.1029/2020JA028763

Wang, Y. Q. (2022). *Snowfall Catalogue from 1625 to 1907 CE in Seoul* [Dataset]. Beijing: WDC for Geophysics. https://doi.org/10.12197/2022GA001

White, W. B., and Liu, Z. Y. (2008). Resonant excitation of the quasi-decadal oscillation by the 11-year signal in the Sun's irradiance. *J. Geophys. Res.: Oceans*, *113*(C1), C01002. https://doi.org/10.1029/2006JC004057

Wigley, T. M. L., and Raper, S. C. B. (1990). Climatic change due to solar irradiance changes. *Geophys. Res. Lett.*, *17*(12), 2169–2172. https://doi.org/10.1029/GL017i012p02169

Xiao, S. B., Li, A. C., Paul Liu, J., Chen, M. H., Xie, Q., Jiang, F. Q., Li, T. G., Xiang, R., and Chen, Z. (2006). Coherence between solar activity and the East Asian winter monsoon variability in the past 8000 years from Yangtze River-derived mud in the East China Sea. *Palaeogeogr. Palaeoclimatol. Palaeoecol.*, *237*(2-4), 293–304. https://doi.org/10.1016/j.palaeo.2005.12.003

Xie, F., Li, J. P., Tian, W. S., Fu, Q., Jin, F. F., Hu, Y. Y., Zhang, J. K., Wang, W. K., Sun, C., … Ding, R. Q. (2016). A connection from Arctic stratospheric ozone to El Niño-Southern oscillation. *Environ. Res. Lett.*, *11*(12), 124026. https://doi.org/10.1088/1748-9326/11/12/124026

Yan, L. M., He, F., Yue, X. N., Wei, Y., Wang, Y. Q., Chen, S., Fan, K., Tian, H., He, J. S., … Xia, L. D. (2023). The 8-year solar cycle during the maunder minimum. *AGU Adv.*, *4*(5), e2023AV000964. https://doi.org/10.1029/2023AV000964

Zhang, Y. C., Jiang, J. W., Jiang, Y. Q., Lu, H. X., Wang, H. Y., Yang, W. Q., Xie, Z. Q., Yan, H., Liu, W. G., and Liu, Z. H. (2024). Solar modulation of the western tropical Pacific hydroclimate over the last ~1200 years. *Quat. Sci. Rev.*, *340*, 108868. https://doi.org/10.1016/j.quascirev.2024.108868

Zhao, L., and Wang, J. S. (2014). Robust response of the East Asian monsoon rainband to solar variability. *J. Climate*, *27*(8), 3043–3051. https://doi.org/10.1175/JCLI-D-13-00482.1

Zhao, L., Wang, J. S., Liu, H. W., and Xiao, Z. N. (2017). Amplification of the solar signal in the summer monsoon rainband in China by synergistic actions of different dynamical responses. *J. Meteor. Res.*, *31*(1), 61–72. https://doi.org/10.1007/s13351-016-6046-6

Zhao, X. H., Soon, W., and Velasco Herrera, V. M. (2020). Evidence for solar modulation on the millennial-scale climate change of Earth. *Universe*, *6*(9), 153. https://doi.org/10.3390/universe6090153

Zhao, X. H., Soon, W., and Velasco Herrera, V. M. (2021). Holocene Millennial-Scale Solar Variability and the Climatic Responses on Earth. *Universe*, *7*(2), 36. https://doi.org/10.3390/universe7020036

Zhu, F. R., and Jia, H. Y. (2018). Lomb–Scargle periodogram analysis of the periods around 5.5 year and 11 year in the international sunspot numbers. *Astrophys. Space Sci.*, *363*(7), 138. https://doi.org/10.1007/s10509-018-3332-z

Zhu, H. F., Fang, X. Q., Shao, X. M., and Yin, Z. Y. (2009). Tree ring-based February–April temperature reconstruction for Changbai Mountain in Northeast China and its implication for East Asian winter monsoon. *Climate Past*, *5*(4), 661–666. https://doi.org/10.5194/cp-5-661-2009